

# On the interface diffusion coefficient for solving Reynolds equation by control volume method

Chung-Jen Lu <sup>\*</sup>, Shean-Son Chiou

*National Taiwan University, Department of Mechanical Engineering, No. 1 Roosevelt Road Sec 4, Taipei 10617, Taiwan*

Received 7 November 2002; received in revised form 17 April 2003; accepted 1 May 2003

## Abstract

When using the control volume method to solve the Reynolds equation, the mass flux crossing the control surface should be calculated properly. According to Pantakar's formulation, which is commonly used in solving general convection–diffusion equations, the mass flux can be expressed as a function of the convection and diffusion coefficients. Consequently, the performance of the numerical algorithm depends strongly on the scheme employed for the calculation of the interface diffusion coefficient. Two diffusion schemes have been proposed in the literature. One scheme (referred to as scheme I) employs the arithmetic mean of the pressure values at the neighboring grid points to evaluate the interface diffusion coefficient, while the other (referred to as scheme II) uses the harmonic mean of the neighbor diffusion coefficients. Scheme I has been used for solving the Reynolds equation successfully. On the other hand, scheme II, while being popular for solving convection–diffusion types of equations when the diffusion coefficient is known, has not been implemented to solve the Reynolds equation for air bearings, in which the diffusion coefficient depends on the unknown dependent variable. In this paper, we implement scheme II for solving the Reynolds equation and compare its performance with that of scheme I. Both numerical and analytical results indicate that scheme II may yield unrealistic results for air bearings with large clearance discontinuities.

© 2003 Elsevier Ltd. All rights reserved.

*Keywords:* Reynolds equations; Gas lubricated bearings; Hard disk drives

## 1. Introduction

The pressure distribution of gas-lubricated bearings is governed by the Reynolds equation, which belongs to the class of convection–diffusion equations. Due to the complex shapes of modern air bearing surfaces, numerical methods have to be employed for solving the Reynolds equation. The control volume method has been successfully applied to solve the convection–diffusion equations [1–3]. When using the control-volume method, it is necessary to calculate the interface fluxes properly. The interface flux can be expressed as a function of the diffusion and convection coefficients at the control surface [3]. For the analysis of air bearings, the interface convection coefficient can be calculated directly from the dimensions of the bearing and the properties of air.

On the other hand, the diffusion coefficient, which depends on the unknown pressure, should be estimated using the values of the dependent variables at neighboring grid points. Two schemes have been proposed to calculate the interface diffusion coefficient. One scheme adopts the harmonic mean of the diffusion coefficients at neighboring grid points as the interface diffusion coefficient; the other scheme uses the arithmetic mean of the pressure values at neighboring grid points for the calculation of the interface diffusion coefficient. Although the former scheme has been implemented successfully for solving convection–diffusion equations when the diffusion coefficient is known, it has not been employed for solving Reynolds equation. In this paper, we apply the harmonic-mean scheme to solve the Reynolds equation and compare its performance with that of the arithmetic-mean scheme.

To this end, we examine a parallel step air bearing. Discretization equations describing the relation between the slope of the pressure at the step and the geometrical

<sup>\*</sup> Fax: +1-886-2-2362-7686.

E-mail address: cjlu@ccms.ntu.edu.tw (C.-J. Lu).

### Nomenclature

$h$	Clearance of the slider
$h_m$	Minimum clearance of the slider
$p$	Pressure
$p_a$	Ambient atmospheric pressure
$u$	Velocity of the moving surface
$x$	Coordinate along the slider
$F$	Convection coefficient ( $= \Lambda H$ )
$H$	Dimensionless clearance
$J$	Flux
$L$	Length of the slider
$P$	Dimensionless pressure
$\tilde{P}$	Peclet number ( $= F\delta/\Gamma$ )
$X$	Dimensionless coordinate
$\delta$	Size of the control volume
$\mu$	Viscosity of the air
$\Lambda$	Bearing number ( $= 6\mu uL/p_a h_m^2$ )
$\Gamma$	Diffusion coefficient ( $= PH^3$ )

configuration of the bearing are derived and analyzed asymptotically. Finally, we present the numerical solutions, which confirm the asymptotic results, and compare the effectiveness of these two schemes.

## 2. Control volume formulation

The steady-state one-dimensional Reynolds equation, which governs the pressure distribution in gas-lubricated bearings, can be written in a non-dimensional form as [4]:

$$\frac{\partial}{\partial X} \left( \Lambda H P - \Gamma \frac{\partial P}{\partial X} \right) = 0, \quad (1)$$

where  $P = p/p_a$ ,  $H = h/h_m$ ,  $X = x/L$ , are the non-dimensionalized pressure, bearing clearance and coordinate in slider length, respectively;  $p_a$  is the ambient atmospheric pressure;  $h_m$  is the minimum clearance;  $L$  is the length of the slider;  $\Lambda = 6\mu u/p_a h_m^2$  is the bearing number and  $u$  is the velocity of the moving surface;  $\Gamma = PH^3$  is the diffusion coefficient.

To obtain the discretization equations, consider a typical control volume as shown in Fig. 1. According to Patankar's formulation [3], the flux across the control surface between grid points  $N-1$  and  $N$  and can be expressed in a compact form as:

$$J = FP_{N-1} + (\Gamma/\delta)A(\tilde{P})(P_{N-1} - P_N), \quad (2)$$

where  $F = \Lambda H$  is the convection coefficient,  $\tilde{P} = F\delta/\Gamma$  is the Peclet number, and  $A$  is a function of the Peclet number. Various schemes can be reached by adopting different function  $A(|\tilde{P}|)$ . In the following analysis, the exponential scheme is used, which is

$$A(|\tilde{P}|) = \frac{|\tilde{P}|}{\exp(|\tilde{P}|) - 1}. \quad (3)$$

Substitution of Eq. (3) into Eq. (2) gives

$$J = F \left( P_{N-1} + \frac{P_{N-1} - P_N}{\exp(\tilde{P}) - 1} \right). \quad (4)$$

By using Eq. (4) and the conservation of flux, we can obtain the discretized equations.

## 3. Interface diffusion coefficient

In Eq. (4), the convection coefficient and Peclet number should be evaluated at the control surface. Therefore we need to know how to determine the interface convection coefficient  $F$  and the diffusion coefficient  $\Gamma$  for computing the flux. The interface convection coefficient is simply the product of the clearance at the control surface and the bearing number. However, the interface diffusion coefficient, which depends on the pressure at the control surface, should be determined by a suitable interpolation scheme. Two schemes, I and II, have been proposed for the calculation of the interface diffusion coefficient. In scheme I [2], the interface diffusion coefficient is calculated as the product of the arithmetic mean of the pressure values of the neighboring grid points and the cube of the clearance at the control surface. In scheme II [3], the harmonic mean of the diffusion coefficients of the neighboring grid points is used as the interface diffusion.

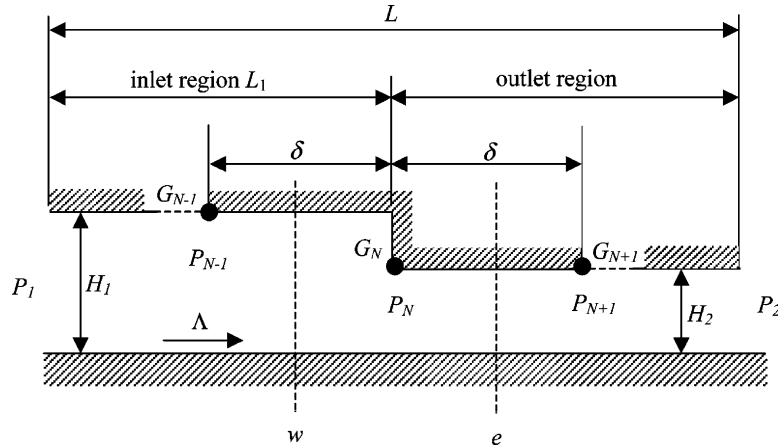


Fig. 1. Parallel-step bearing and a typical control volume surrounding  $G_N$ .

### 4. Discretized equation

A parallel step gas bearing is used in this study to compare the performance of these two diffusion schemes. Fig. 1 illustrates the geometry and boundary conditions of the step gas bearing. According to Lu's results on shaped-rail sliders [2], the grid points should be assigned to the clearance discontinuities to reduce the numerical errors. Therefore we place a grid point, say  $G_N$ , at the step. Consider a typical control volume surrounding  $G_N$  (Fig. 1). The flux across each of the control surfaces is determined using Eq. (4). Note that the Peclet number is proportional to the size of the control volume. In the following analysis, we assume that the control volume is sufficiently small so that

$$\exp(\tilde{P}) \approx 1 + \tilde{P} \tag{5}$$

and

$$P_{N-1} = P_N + o(\delta), \tag{6}$$

where  $\delta$  is the size of the control volume. Then we derive the discretized equations for this control volume using the two diffusion schemes, respectively.

In scheme I, the diffusion coefficient on the control surface  $w$  is calculated as

$$\Gamma_w = (P_{N-1} + P_N)H_1^3/2, \tag{7}$$

and the corresponding Peclet number is

$$\tilde{P}_w = \frac{2\Lambda\delta}{(P_{N-1} + P_N)H_1^3}. \tag{8}$$

Incorporating Eqs. (5)–(8) into Eq. (4) gives

$$J_w = \Lambda H_1 P_N + P_N H_1^3 \left( \frac{P_{N-1} - P_N}{\delta} \right). \tag{9}$$

A similar expression can be written for the flux crossing the east control surface  $e$ :

$$J_e = \Lambda H_2 P_N + P_N H_2^3 \left( \frac{P_N - P_{N+1}}{\delta} \right). \tag{10}$$

From the conservation of mass flux,  $J_e = J_w$ , we obtain the following expression

$$\frac{P_{N-1} - P_N}{\delta} = \frac{\Lambda}{H_1^2} \left( \frac{H_2}{H_1} - 1 \right) + \left( \frac{H_2}{H_1} \right)^3 \left( \frac{P_N - P_{N+1}}{\delta} \right). \tag{11}$$

In scheme II, the interface diffusion coefficient is calculated as the harmonic mean of the diffusion coefficients on the neighboring grid points and hence depends on the clearances at the neighboring grid points. In order to simplify the data structure and the associated numerical algorithm, we use a single-clearance method, i.e. only one value of clearance can be assigned to each node. The clearance  $H_N$  of grid point  $G_N$ , which is located at the step, can be set as either  $H_1$  or  $H_2$ . We consider the case  $H_N = H_2$  first and derive the result for  $H_N = H_1$  later. For the case  $H_N = H_2$ , the diffusion coefficient at the west control surface  $w$  is

$$\frac{1}{\Gamma_w} = \frac{1}{2} \left( \frac{1}{P_{N-1} H_1^3} + \frac{1}{P_N H_2^3} \right). \tag{12}$$

Consequently, the corresponding Peclet number is

$$\tilde{P}_w = \frac{\Lambda H_1 \delta}{2} \left( \frac{1}{P_{N-1} H_1^3} + \frac{1}{P_N H_2^3} \right). \tag{13}$$

Substituting Eq. (13) into Eq. (4), using Eqs. (5) and (6), yields

$$J_w = \Lambda H_1 P_N + \frac{2P_N}{1/H_1^3 + 1/H_2^3} \left( \frac{P_{N-1} - P_N}{\delta} \right).$$

In a similar manner, the flux across control surface  $e$  can be written as

$$J_e = \Lambda H_2 P_N + P_N H_2^3 \left( \frac{P_N - P_{N+1}}{\delta} \right).$$

Conservation of mass flux requires that  $J_e = J_w$ , and hence

$$\frac{P_{N-1} - P_N}{\delta} = \frac{1/H_1^3 + 1/H_2^3}{2} \quad (14)$$

$$\left[ \Lambda(H_2 - H_1) + H_2^3 \left( \frac{P_N - P_{N+1}}{\delta} \right) \right]$$

For the case  $H_N = H_1$ , following the procedure shown above, we can obtain

$$\frac{P_{N-1} - P_N}{\delta} = \frac{\Lambda(H_2}{H_1^2(H_1 - 1)} \quad (15)$$

$$+ \frac{2}{1 + (H_1/H_2)^3} \left( \frac{P_N - P_{N+1}}{\delta} \right).$$

**5. Asymptotic analysis**

In this section, we discuss the results of schemes I and II for step bearings with large values of clearance ratio.

We consider converging step bearings ( $H_1 > H_2 = 1$ ) first. For large values of the inlet clearance, i.e.  $H_1 \gg 1$ , the step bearing will asymptotically reduce to a parallel bearing with length  $(L - L_1)$  and clearance  $H_2$ . In these cases, the pressure in the inlet region would approach the ambient pressure and the pressure at the step will be somewhat higher than the ambient pressure. Consequently, the left-hand slope of the pressure at the step would be a very small value and the right-hand slope would be somewhat less than zero. For scheme I, as can be seen from Eq. (11), the left-hand pressure slope at the step approaches zero for  $H_1 \gg 1$ , as expected. For scheme II, the result depends on  $H_N$ , the clearance at  $G_N$ . For  $H_N = H_2$ , the left-hand slope increases with  $H_1$  as shown by Eq. (14). This indicates an unrealistic large left-hand slope for  $H_1 \gg 1$ . In contrast, for  $H_N = H_1$ , the left-hand slope approaches zero for  $H_1 \gg 1$  (see Eq. (15)).

The same arguments as above can be applied to diverging step bearings ( $H_2 > H_1 = 1$ ) with large values of the outlet clearance. For  $H_2 \gg 1$ , the pressure at the step will be somewhat lower than the ambient pressure and the left-hand slope of the pressure at the step would be a small value. Because  $P_N < P_{N+1}$ , the two terms on the right-hand side of Eqs. (11) and (14) both increase with  $H_2$  but with different signs. Under these conditions, we cannot draw any conclusion regarding the magnitude of the left-hand slope from Eqs. (11) and (14). In contrast, Eq. (15) indicates that the left-hand slope increases with  $H_2$ , which leads unrealistic results for  $H_2 \gg 1$ .

The above discussion leads to the conclusion that scheme II may produce unrealistic solutions for gas bearings with large clearance discontinuities.

**6. Results and discussion**

The step bearing shown in Fig. 1 is used to study the performance of these two diffusion schemes. We calculate the pressure distribution for different inlet/outlet clearances. The other parameters are kept at fixed values as follows:  $L = 1$ ,  $L_1 = 0.5$ ,  $P_1 = P_2 = 1$  and  $\Lambda = 30$ . Analytical solutions of the pressure distribution under these conditions can be found in Burgdorfer [5].

Recall that the results of scheme II depend on the clearance  $H_N$  at the grid point  $G_N$ . For the brevity of discussion, let schemes II<sub>L</sub> and II<sub>R</sub> denote the cases of  $H_N = H_1$  and  $H_N = H_2$ , respectively. Fig. 2 shows the pressure profiles obtained using scheme I and scheme II when  $H_1 = 2$  and  $H_2 = 1$ . Here, 75 grid points are used. As can be seen from the figure, the pressure distributions obtained from scheme I and scheme II<sub>L</sub> agree well with the analytical solution. On the other hand, scheme II<sub>R</sub> overestimates the pressure in the inlet region ( $x > 0.5$ ) and underestimates it in the outlet region ( $x < 0.5$ ). There are considerable deviations from the analytical solution around the step. Consequently, the left-hand slope of the pressure at the step obtained using scheme II<sub>R</sub> is much higher than the exact value. Also note that the slope for scheme II<sub>R</sub> is discontinuous at the node immediately before the step. According to the asymptotic analysis presented in the previous section, these problems are due to the improper use of harmonic mean for the calculation of the flux crossing the control surface immediately before the step. Figure 3 presents comparisons between the left-hand slopes at the step for different grid sizes obtained using schemes I and II<sub>R</sub>. For scheme I, the results agree well with the exact value, 3.74, for grid sizes larger than 25. On the other hand, the left-hand slope obtained using scheme II<sub>R</sub> increases with grid size and converges to a value much higher than the exact value. Then we study the effects of the clearance ratio ( $H_1/H_2$  for converging bearings and  $H_2/H_1$  for diverging

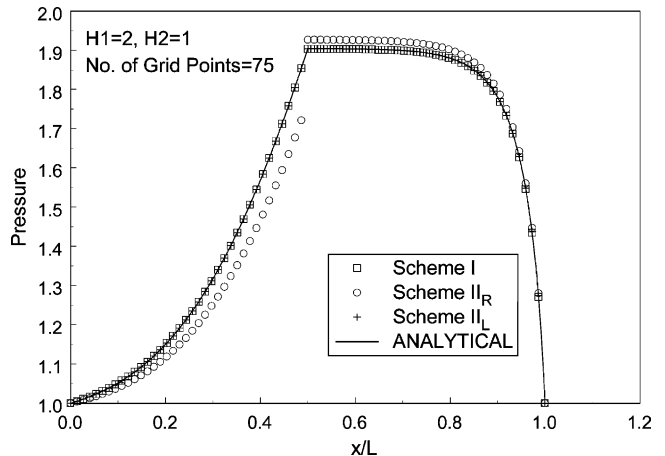


Fig. 2. Comparison of pressure profiles calculated using schemes I and II with the analytic solution.

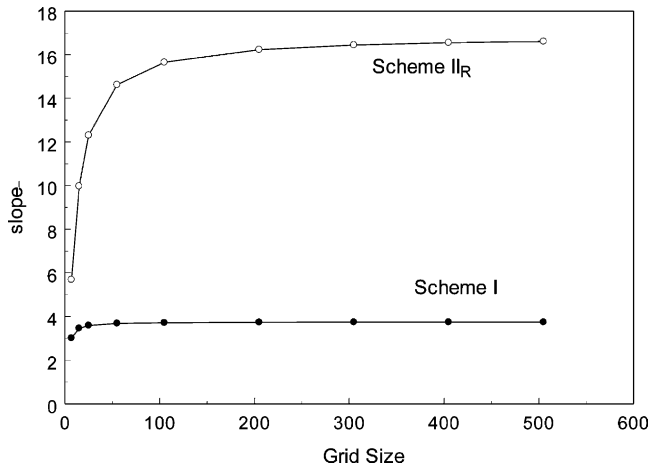


Fig. 3. Left-hand slope at the step vs. grid size ( $H_1 = 2$ ,  $H_2 = 1$ ).

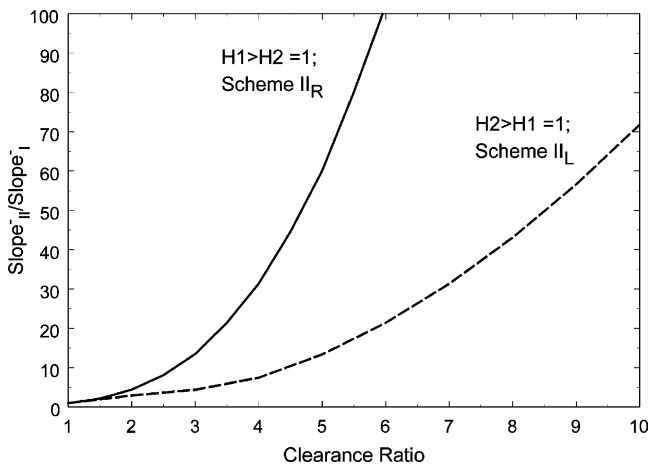


Fig. 4. Effect of clearance ratio on the left-hand slope at the step calculated using scheme II.

bearings) on the left-hand slope at the step. The results are shown in Fig. 4, where the solid line denotes the case  $H_1 > H_2 (= 1)$  and the dashed line indicates the case  $H_2 > H_1 (= 1)$ . Schemes II<sub>R</sub> and II<sub>L</sub> are used for the cases  $H_1 > H_2$  and  $H_2 > H_1$ , respectively. Slope<sub>I</sub> indicates the left-hand slope calculated using scheme I. As can be seen from the figure, scheme II greatly overestimates the left-hand slope for both cases and the relative error increases with the clearance ratio. These results agree with the asymptotic analysis presented in the previous section.

The problem encountered when using scheme II may be remedied by employing a multi-clearance method as proposed by Peng and Hardie [6]. In this method, two values of clearance are associated with the grid point  $G_N$  located at the step (see Fig. 1). When calculating the

diffusion coefficient at control surface  $w$ , the clearance of  $G_N$  is set as  $H_1$  because most of the section between nodes  $G_{N-1}$  and  $G_N$  is at the height  $H_1$ . Similarly, the clearance at node  $G_N$  should be set to be  $H_2$  when computing the diffusion coefficient at control surface  $e$ . This method indeed yields correct pressure profiles at the discontinuities. However, in the multi-clearance method, the data structure associated with each node and the corresponding numerical algorithm are much more complex than those with single-clearance method.

## 7. Conclusions

This paper presents a comparison study of the performance of two diffusion schemes, referred to as scheme I and scheme II, used for solving the Reynolds equation via the control volume method. Scheme I employs the arithmetic pressure values at neighboring grid points to calculate the interface diffusion coefficient. In scheme II, the harmonic mean of the diffusion coefficients at neighboring grid points is used as the interface diffusion coefficient. A parallel step bearing is used to compare the effectiveness of these two diffusion schemes. Numerical results obtained using scheme I agree well with the analytical solutions. In contrast, scheme II highly overestimates the slope of the pressure at the step, as predicted by the asymptotic analysis.

## Acknowledgements

This research was supported by the National Science Council of the Republic of China under grant No. NSC-89-2212-E-002-109.

## References

- [1] Cha E, Bogy DB. A numerical scheme for static and dynamic simulation of subambient pressure shaped rail sliders. *ASME Journal of Tribology* 1995;117:36–46.
- [2] Lu S. Numerical simulation of slider air bearings. Doctoral dissertation, Department of Mechanical Engineering, University of California, Berkeley, 1997.
- [3] Patankar SV. Numerical heat transfer and fluid flow. New York: McGraw-Hill, 1980.
- [4] Hamrock BJ. Fundamentals of fluid film lubrication. New York: McGraw-Hill, 1994.
- [5] Burfordorfer A. The influence of the molecular mean free path on the performance of hydrodynamic gas lubricated bearings. *ASME Journal of Basic Engineering* 1959;94:100.
- [6] Peng JP, Hardie CE. A finite element scheme for determining the shaped rail slider flying characteristics with experimental confirmation. *ASME Journal of Tribology* 1995;117:358–64.